



# Nested intrashelf platform clinoforms—Evidence of shelf platform growth exemplified by Lower Cretaceous strata in the Barents Sea

Ivar Midtkandal<sup>1</sup>  | Thea Sveva Faleide<sup>1</sup> | Jan Inge Faleide<sup>1,2</sup>  | Sverre Planke<sup>2,3</sup>  | Ingrid Anell<sup>1</sup> | Johan Petter Nystuen<sup>1</sup>

<sup>1</sup>Tectonostratigraphic Research Group, Department of Geoscience, University of Oslo, Oslo, Norway

<sup>2</sup>Centre for Earth Evolution and Dynamics (CEED), Department of Geosciences, University of Oslo, Oslo, Norway

<sup>3</sup>Volcanic Basin Petroleum Research, Oslo Innovation Center, Oslo, Norway

## Correspondence

Ivar Midtkandal, Tectonostratigraphic Research Group, Department of Geoscience, University of Oslo, Oslo, Norway.

Email: ivar.midtkandal@geo.uio.no

## Funding information

ARCEX, Grant/Award Number: 228107

## Abstract

Two nested clinoform set types of different scales and steepness are mapped and analysed from high-resolution seismic data. Restoration of post-depositional faulting reveals a persistent pattern of small-scale, high-angle clinoforms contained within platform-scale, low-angle clinoforms, showing a combined overall progradational depositional system. The large clinoforms lack a well-defined platform edge, and show a gradual increase in dip from topset to foreset. A consistent recurring stratal pattern is evident from the architecture, and is considered a result of interplay between relative sea-level change and autocyclic switching of sediment delivery focal points that brought sediment to the platform edge. This un-interrupted succession records how intra-shelf platforms prograde. Quantitative clinoform analysis may assist in determining the most influential depositional factors. Post-depositional uplift and erosion requires restoration with re-burial to maximum burial depth. Backstripping, decompaction and isostatic correction was performed assuming a range of lithologic compositions, as no wells test the lithology. Nearby wells penetrate strata basinward of the clinoforms, proving mudstone content above 50%, which in turn guide restoration values. Typical restored platform heights are 250–300 m, with correspondingly sized platform-scale clinoform heights. Typical large-scale clinoform foreset dip values are 1.3°–2.4°. Small-scale clinoforms are typically 100 m thick, with restored foreset dip angles at 4.4° → 10°. The results suggest that intrashelf platform growth occurs in pulses interrupted by draping of strata over its clinoform profile. The resultant architecture comprises small-scale clinoforms nested within platform-scale clinoforms.

## KEYWORDS

clinoform, intracratonic basins, sedimentology, sediment burial and decompaction, stratigraphy

This is an open access article under the terms of the Creative Commons Attribution License, which permits use, distribution and reproduction in any medium, provided the original work is properly cited.

© 2019 The Authors. Basin Research published by International Association of Sedimentologists and European Association of Geoscientists and Engineers and John Wiley & Sons Ltd.

## 1 | INTRODUCTION

Seismic stratigraphic analysis of clinothem successions is a proven tool to constrain depositional history dynamics of basin margins, both onshore and offshore (e.g., Patruno & Helland-Hansen, 2018). A single clinoform depicts a bathymetric profile that developed in response to sediment transport and dispersal mechanisms at a given time. The rock volume between successive clinoforms, termed clinothem, is the depositional product of those processes.

Clinoforms develop at a range of scales, from >1 km high continental margin profiles, to less than 10 m high delta mouth bar units at the shoreline (e.g., Helland-Hansen & Hampson, 2009; Patruno, Hampson, & Jackson, 2015). Shelf prisms (*sensu* Patruno et al., 2015), or intrashelf platforms (*sensu* Mountain & Proust, 2010) are a few 100-m high and develop within continental shelves, and constitute significant sediment volumes that are delivered into the basin beyond shoreline deltas, or during low relative sea-level when the shoreline is displaced basinward. Intrashelf platforms are differentiated from subaqueous deltas in Patruno et al. (2015) as larger features that develop in a distal position from the subaqueous delta component, and are not always developed or discernible on seismic data. Subaqueous delta clinoforms are reported to represent an intermediate scale between shoreline deltas and shelf platform, but there are overlapping values when comparing schematic representations of hierarchical breakdowns of clinoform sizes (see Patruno et al., 2015; Figure 1).

The conventional subdivision of a clinoform's components constitutes a low-angle topset and bottomset, separated by a steeper foreset component, with the point of maximum curvature between the topset and foreset commonly termed the rollover point, platform edge, or shelf edge, depending on context and scale (Patruno & Helland-Hansen, 2018). Successive clinoforms reflect how progradation of sediments into a basin occurred. Any relative changes in appearance between successive clinoforms is a representation of changes in depositional conditions such as sediment influx rate, water depth, sediment composition and character, and physical processes acting on the sea floor.

Recent studies have quantitatively analysed clinoforms in an effort to use their geometric expressions as a proxy to determine lithologies and thereby reservoir potential (e.g., Anell & Midtkandal, 2017; Patruno & Helland-Hansen, 2018). For example, Patruno et al. (2015) noted that the foreset dip-angles of shelf-prism clinoforms are 0.6°–4.7°, without reference to lithology.

Accurate description and interpretation of clinoforms' geometric attributes relies on seismic resolution coupled with accurate acoustic velocity information about the strata in question. Restoration of clinoform dip-angles also requires reliable palaeo-horizontal datum surfaces. Additionally, the

### Highlights

- A two-order nested architecture of clinoforms is identified.
- High-angle clinoforms are documented within platform-scale clinothem.
- High-resolution seismic provides improved shelf platform growth insights.
- Lithologic differences along a progradational dip section complicates decompaction.

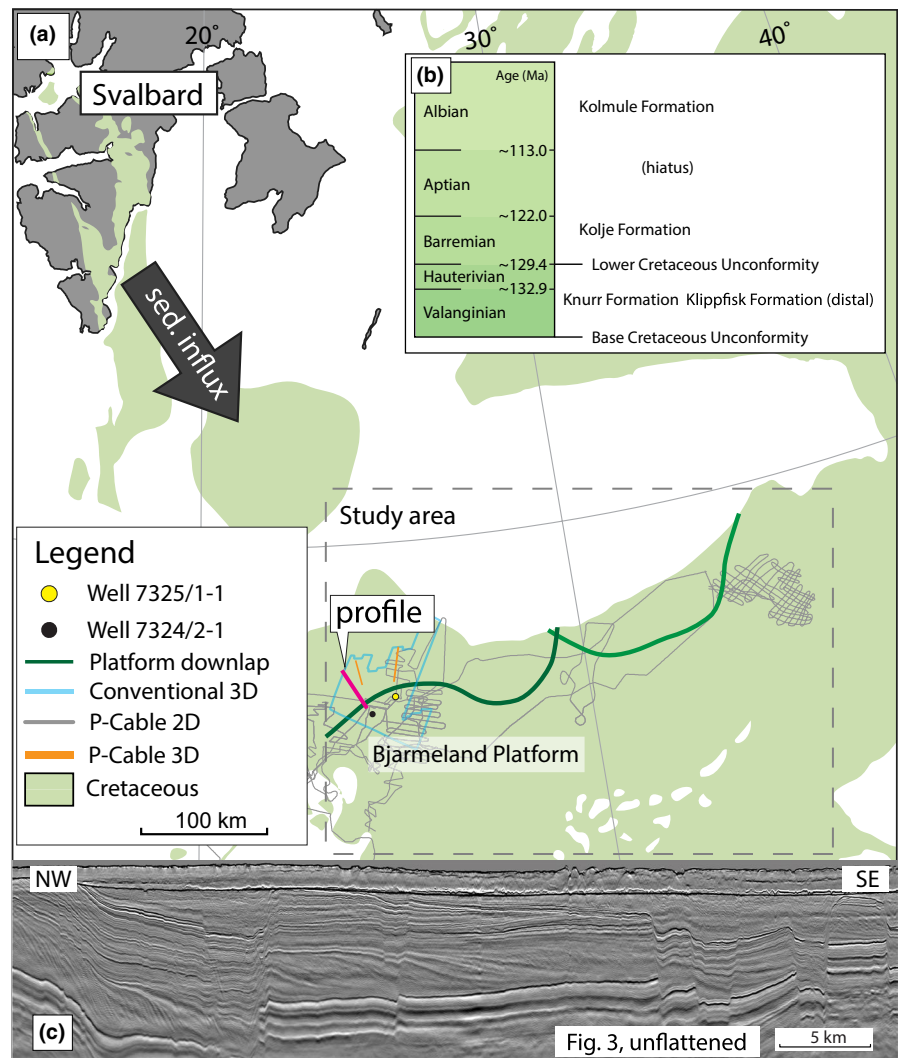
present-day observed geometries of the buried clinoforms have to be backstripped and restored to time of deposition, taking into account the effects of post-depositional compaction and differential loading during burial.

This study is focused on a Cretaceous succession on the Bjarmeland Platform, southwestern Barents Sea (Figure 1a). The succession is imaged in conventional and high-resolution seismic data. The aim is to provide a detailed description of the clinoform architecture based on a method for accurate reconstruction of their internal geometries involving backstripping and decompaction from maximum burial followed by an isostatic correction for differential loading effects according to lithologic composition, and to discuss their development in light of their restored geometric expression.

## 2 | GEOLOGICAL SETTING—THE BOREAL BASIN AND THE BARENTS SEA

The studied succession belongs to the Kolje Formation of inferred Barremian-Aptian age (Worsley, Johansen, & Kristensen, 1988), the most distal component of a fluvial to marine sediment routing system running from NW to SE (Figure 1a, b) in response to a regional forced regression (Døssing et al., 2013; Midtkandal & Nystuen, 2009). The corresponding onshore strata on Svalbard are the Helvetiafjellet and Carolinefjellet formations, mapped as fluvial to tidally influenced marginal marine, to storm-influenced open marine shelf strata (Grundvåg et al., 2017). Cenozoic uplift and erosion has removed around 2,200–2,400 m of the stratigraphic record in the area (Baig, Faleide, Jahren, & Mondol, 2016; Henriksen et al., 2011), and the preserved strata can be imaged at very high resolution with P-Cable technology due to their present shallow burial depth (Lebedeva-Ivanova et al., 2018). The strata represent intrashelf clinothem that prograded into the epicontinental Boreal Basin towards SE (Midtkandal et al., in press). The Kolje Formation developed partly as a prograding shelf platform in the Bjarmeland Platform area (Figure 1c), and also

**FIGURE 1** (a) Map of the western Barents Sea, with study area and seismic data coverage. Conventional 2D data grid is not shown, as it would obscure the other data. Note that the P-Cable 3D volumes are very narrow, and appear as lines on the map. (b) Lithostratigraphy with ages and key horizons. (c) Unflattened seismic profile (labeled) shown in Figure 3a, b. Seismic data courtesy of TGS, WGPS, and VBPR



includes its distally equivalent and horizontally layered undifferentiated marine strata (not studied here). It is mudstone-rich based on available well data from adjacent areas.

The Valanginian-Hauterivian Knurr and Klippfisk formations (Smelror, Larssen, Olaussen, Rømuld, & Williams, 2019; Smelror, Mørk, Monteil, Rutledge, & Leereveld, 1998) form the substrate onto which the clinoform-bearing strata prograded. They are dominantly open marine horizontally layered mudstones (Knurr Fm.) that transition into open marine platform carbonates towards SE (Klippfisk Fm.). The Kolmule Formation overlies the Kolje Formation (Figure 1b).

### 3 | SEISMIC DATA AND ANALYSIS

A grid with 2–5 km line spacing of conventional 2D seismic survey profiles cover the entire study area (Figure 1). A 3D volume of conventional seismic data covers a portion of the western study area, and is used to calibrate true dip direction observations from 2D high-resolution data (details in Corseri et al., 2018; Midtkandal et al., in press). A composite

high-resolution 2D line covers parts of the study area, and is complemented by two small 3D P-Cable volumes (Figure 1a) (resolution details in Corseri et al., 2018; Lebedeva-Ivanova et al., 2018). The high-resolution 2D line forms the most important data set in this study. No wells penetrate the clinothem succession in the Kolje Formation, but the wells 7324/2-1 (Apollo) and 7325/1-1 (Atlantis) drilled the horizontally layered strata less than 5 km SE of the youngest clinoform topset (Figure 1a). Age data beyond a general Barremian-Aptian dating of the whole platform succession is non-existent, preventing any sediment accumulation rate analysis.

Restoration of strata to their original depositional volumes is necessary in order to calculate thickness and dip-angles correctly. The method for accurately restoring the clinoforms/clinothems to their correct geometric and volumetric expression immediately following deposition is as follows:

#### 3.1 | Flattening and fault restoration

Post-depositional faulting and erosion impedes tracing of palaeo-horizontal surfaces above the clinoforms with

confidence. Most reflectors curve gradually from topset position towards the downlap point (Figure 3a, b), and thus only function as horizontal datum surfaces in their most proximal (NW) portions, but remain unfit for flattening of successive clinothem sets, the preferred method in Klausen and Helland-Hansen (2018). The basin floor that the platform prograded onto is assumed to have been close to horizontal and smooth at the time of deposition (Midtkandal & Nystuen, 2009). Flattening along this clinoform downlap surface restores local topset surfaces back to a sub-horizontal position parallel to the downlap surface. This validates the downlap surface as a palaeo-horizontal datum for this study and roughly restores faults within the sediment volume. This fault-restoration by flattening creates zones around the faults that may appear as disturbed stratigraphy (marked on Figure 3a).

### 3.2 | Backstripping and decompaction

Clinoform backstripping and decompaction from maximum burial is necessary for calculations of original height and dip, after corrections for exhumation since maximum burial is performed. The decompaction follows the principles of Allen and Allen (2013), building on the classical paper by Sclater and Christie (1980). With this approach, correct decompaction can only be attained through considering the maximum burial depth at which the unit has been buried, and then decompacting accordingly:

$$y'_2 - y'_1 = y_2 - y_1 - \frac{\varphi_0}{c} \{e^{-cy_1} - e^{-cy_2}\} + \frac{\varphi_0}{c} \{e^{-cy'_1} - e^{-cy'_2}\} \quad (1)$$

In Equation 1,  $y'_2$  is the base decompacted layer;  $y'_1$  is top decompacted layer;  $y_2$  is the base layer at maximum burial;  $y_1$  is the top layer at maximum burial;  $\varphi_0$  represents the surface porosity; and  $c$  is the porosity-depth coefficient. The top of the decompacted layer is assumed to be at zero ( $y'_1 = 0$ ), for simplicity.  $y'_2 - y'_1$  is thus the decompacted thickness ( $h_2$  in Figure 2) of a target feature. The surface porosity and the porosity-depth coefficient vary according to the shale and sand content. In this case, the values for 90% shale ( $\varphi_0 = 0.61$ ,  $c = 0.48$ ), 50/50% shale-sand ( $\varphi_0 = 0.56$ ,  $c = 0.39$ ) (Allen & Allen, 2013; Rüpke, Schmalholz, Schmid, & Podladchikov, 2008; Sclater & Christie, 1980) are applied.

Decompaction increases the height of the clinoforms and consequently the restored dip angles. At present, the studied clinoforms are located a few hundred metres and less below the seabed, but prior to Late Cenozoic uplift and erosion they were buried ~2,300 m deeper (Baig et al., 2016; Henriksen et al., 2011). The maximum burial depth for top Kolje Formation ( $y_1$ , Equation 1) is estimated to be the sum of net erosion and the present day Kolmule Formation thickness (2,300 m + 150 m = 2,450 m) (Figure 2). A seismic velocity of 2,900 m/s is measured for the Kolje Formation in well 7324/2-1 (Figure 1a), and is used for depth-conversion of the target strata, excluding present-day water depth (~400 m) (Figure 3). This velocity is typical also for mudstones at present-day maximum burial depths of 2,200–2,500 m, with ~20% porosity in the North Sea (Marcussen, Faleide, Jahren, & Bjørlykke, 2010), validating the values applied here. Using

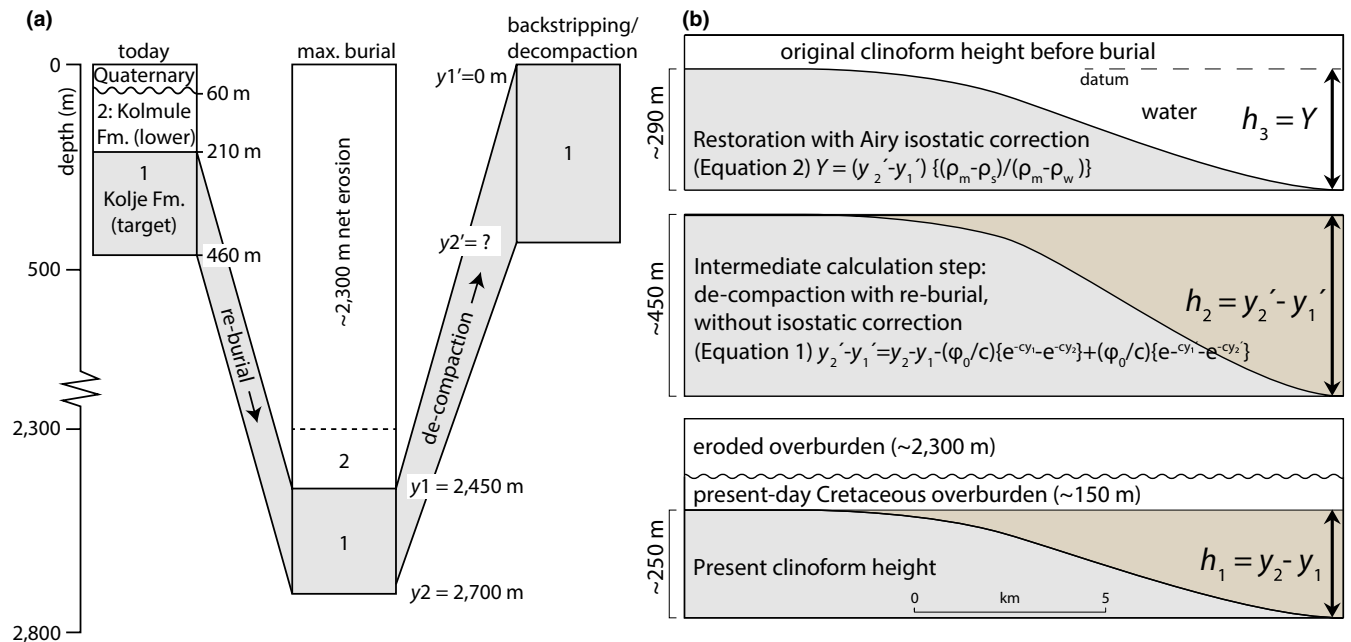


**FIGURE 2** (a) Sediment thickness restoration method, with decompaction from maximum burial depth where 2,300 m eroded section has been added based on Henriksen et al. (2011) and Baig et al. (2016). (b) Calculation steps from present burial depth (bottom), via an intermediate calculation step that restores thickness from maximum burial depth according to lithologic decompaction coefficients (middle), and Airy isostatic correction (top)

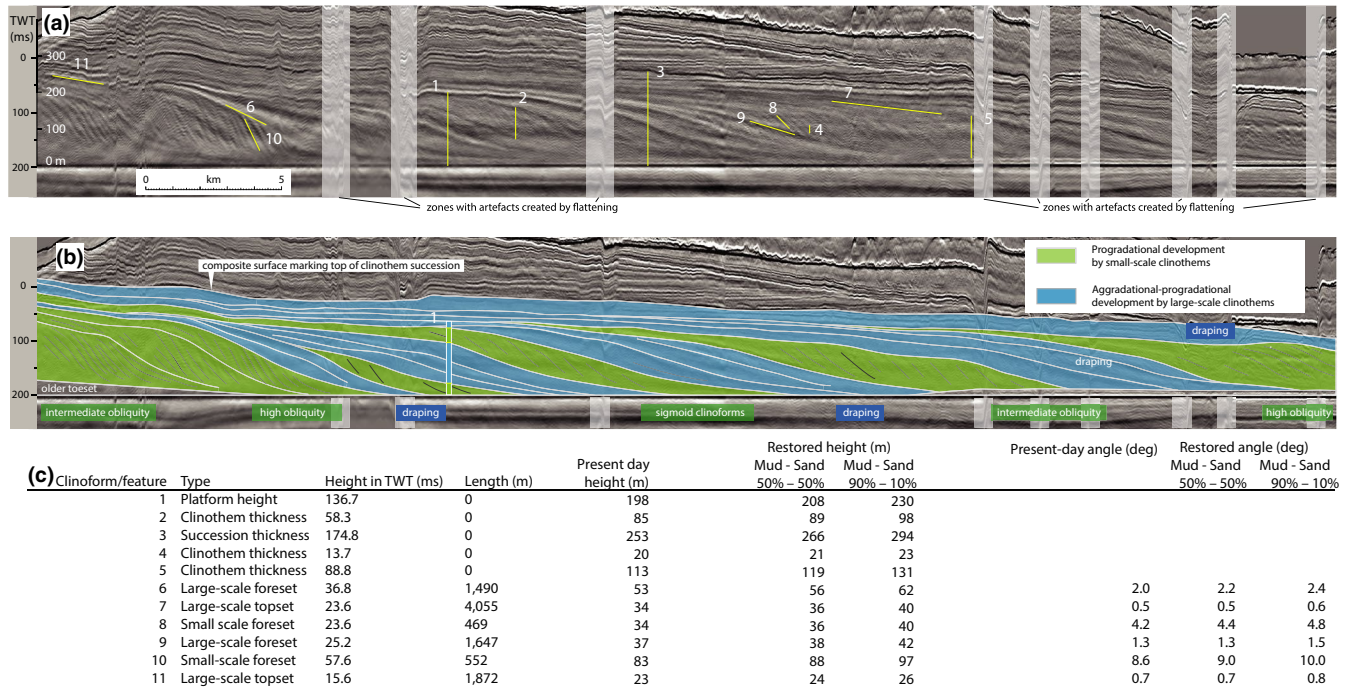


**FIGURE 3** (a) Seismic profile from Figure 1c, flattened along common large-scale clinoform downlap surface for restoration of post-depositional faulting. Yellow numbered lines are features detailed in table at bottom. Note marked areas with artefacts near faults. (b) Seismic profile with interpretations, showing small-scale, high-angle clinoforms, and platform-scale, low-angle clinoforms. (c) Measured and restored stratigraphic thicknesses and dip angles from selected features in profile above. Seismic data courtesy of TGS, WGPS, and VBPR

this velocity, it is also assumed that the thickness at maximum burial is equal to the present-day thickness.

### 3.3 | Effect of differential loading and Airy isostasy

Restoration of a clinoform to its original dimensions and geometry also requires isostatic compensation for the differential load above the clinoform (Allen & Allen, 2013). Neglecting this will lead to exaggerated relief and overestimated dip angles. Accounting for isostatic subsidence related to differential loading reduces the decompaction effect. Airy isostasy is calculated according to:

$$Y = (y'_2 - y'_1) \left\{ \frac{\rho_m - \rho_s}{\rho_m - \rho_w} \right\} \quad (2)$$

$Y$  in Equation 2 is the depth to base of the target feature after correction for decompaction and Airy isostasy. Decompaction was calculated by applying the thickness ratio between restored ( $h_3$  in Figure 2) and present-day thicknesses ( $h_1$  in Figure 2), and applied to target depth-converted heights in the profile (Figure 3). Assuming a 90% mudstone lithology, the restored clinoform height, based on backstripping, decompaction and Airy isostatic correction for differential

loading (Allen & Allen, 2013) increases by ~16% compared to the measured thickness of the present buried clinothem, while ~5% increase is restored from 50/50% sandstone/mudstone (Figure 2). Error ranges are calculated from maximum and minimum values for  $V_p$  (2,800–3,000 m/s), sediment density (1,750–1,950 kg/m<sup>3</sup>), mantle density (3,200–3,400 kg/m<sup>3</sup>), and erosion estimates (2,200–2,400 m). These ratios were used for the restoration of stratigraphic thicknesses, and thereby calculation of the original dips of selected clinoforms. Ideally, the clinoform geometries should be restored by a 2D basin modelling tool, which in addition to the backstripping and decompaction take into account eustatic sea level and paleobathymetry, as well as testing effects of differential loading for both Airy and flexural isostasy. However, such an approach is beyond the scope of this short paper.

## 4 | DEPOSITIONAL CHARACTERISTICS

The open marine shelf platform clinoforms pictured in Figure 3a, b developed an unknown distance from the contemporary shoreline. Two clinoform scales are discernible within the high-resolution seismic data. The selected seismic profile (Figure 3a, b) is oriented sub-parallel to the sediment transport direction, and thus exhibits close to maximum clinoform

dip angles. The observations are organized according to the two scales of clinoform architecture; one large-scale clinoform set matches the total height of the sedimentary succession, and smaller sets contained within some of the large-scale clinoforms.

The large-scale clinoforms are aggradational-progradational, platform-sized features that exhibit a generally well preserved topset—foreset—toeset sigmoid shape with relatively low foreset angles compared to the small-scale features (described below) (Figure 3). Several clinoforms lack a well-defined platform edge where the sub-horizontal topset component meets a steeper foreset in a well-defined rollover. Instead, the transition is gradual, shown as increasing topset divergence, and makes identification of the platform edge problematic. The corresponding large-scale clinoforms drape the entire platform, and some contain small-scale clinoforms and clinoforms within them (Figure 3a, b). Even without readily identifiable platform edge points, the shelf edge trajectory is flat to rising, as the topsets are largely preserved. The total platform height and its corresponding clinoforms decrease slightly towards SE, suggesting an overall falling trajectory. Typical foreset dip values range between  $1.3^\circ$  and  $2.2^\circ$  ( $\pm 0.3^\circ$ ) for 50% mudstone/sandstone, and  $1.5^\circ$ – $2.4^\circ$  ( $\pm 0.3^\circ$ ) for 90% mudstone; 10% sandstone (Figure 3). Tilted topset dip-angles range around  $0.8^\circ$  ( $\pm 0.01^\circ$ ) for both 50% and 90% mudstone restoration values (Figure 3c). Clinoform thicknesses vary depending on picked surfaces and interpretation. The clinoform marked as no. 2 in Figure 3a restores to 89 m for 50% mudstone composition, and 98 m for 90% mudstone.

Small-scale clinoforms are contained within large-scale clinoforms, and are only visible in the high-resolution seismic data. They downlap onto large-scale clinoforms, or onto the basin floor. Their corresponding toplap surfaces are generally defined by the overlying large-scale clinoform surface, which ultimately laps down onto the basin floor further into the basin. Topsets are preserved in the youngest small-scale clinoforms (Figure 3). Their parent clinoform is typically sigmoid (incremental thickness increase followed by decrease). Small-scale clinoforms show varying degrees of obliquity between successive sets, while single sets retain a consistent obliquity (Figure 3b). The small clinoforms are generally steeper than their bounding large-scale clinoforms, and exhibit straight and parallel foresets. Small-scale foreset angles range from  $4.4^\circ$  to  $10.0^\circ$  ( $\pm 1.0^\circ$ ) depending on restoration (Figure 3c) (note that  $10.7^\circ$  is considered steeper than what is considered possible for intrashelf clinoforms by Patruno et al., (2015)). Their downlap terminations, relatively poorly resolved in the seismic data, appear abrupt and high-angled compared to the large-scale clinoforms. There is no discernible evidence of significant topset erosion directly above, or in their proximal contemporaneous strata.

## 5 | DISCUSSION: CLINOFORM DEVELOPMENT AND SHELF PLATFORM GROWTH

The periods represented by aggradational to progradational development of large-scale clinoforms either reflect marine flooding, or periods when the sediment delivery focal point was offset from the basin site represented by the trajectory recorded in the seismic profile (Figure 3). A flat to rising rollover trajectory coupled with overall platform height decrease reflects early, syn-sedimentary compaction. The draping strata contributed significantly to the platform growth, both vertically and basinward, despite the absence of small-scale clinoforms, and is another example of muddy platform growth by sediment delivery to the platform margin by storm agitation of shelf platform mud (Poyatos-Moré et al., 2016). If the draping strata developed while small-scale clinoforms prograded in a lateral position along the platform front, it may imply a greater lithologic contrast between the small-scale clinoforms and the platform-scale clinoforms. As noted above, restoration of the steepest foresets according to 90% mudstone composition yields gradients that are very close to what is considered unrealistic (Patruno et al., 2015), suggesting these clinoforms may contain more than 10% sandstone. In this scenario, coarser material was probably delivered to and across the platform edge in one area, causing it to prograde rapidly, while sediment partitioning caused mud to accumulate elsewhere. This may reflect a variable shelf platform width along the shelf platform strike, such as suggested in Jones, Hodgson, and Flint (2015), which is conceivable when considering the lobate downlap front as mapped by Midtkandal et al. (in press) (Figure 1a).

The small-scale clinoforms' characteristic and consistent steep and straight foresets coupled with abrupt, high-angle downlap terminations suggest that accumulation of sediment along the platform front (i.e., progradation) occurred by gravitational sediment transport. The small-scale clinoforms are consequently assumed to consist of mass-flow products. Consistent obliquity within successions is indicative of a common progradation direction during their development. Consistent lithologic variation in mudstone:sandstone ratio within the sets is a likely cause of their well-defined seismic resolution, which may stem from high-frequency pulses of accumulation coupled with abandonment. The origins of the two orders of sediment influx rate recorded in the data cannot be determined to represent specific forcing mechanisms without information on duration and their lithological composition.

The observed lowering towards the basin floor of the topset surface belonging to the small-scale clinoforms is enigmatic. Considering their toplap surface is a clinoform foreset itself in several places, a horizontal restoration of this surface can be ruled out. If these clinoforms are platform-edge

deltas (shelf-edge deltas *sensu* Patruno & Helland-Hansen, 2018), it implies the improbable scenario that they recorded a relative sea-level fall that matched the full platform height (>250 m) several times during the platform growth. This is supported by the absence of any discernible erosional scours at the rollover zone or in the topset strata. A more likely explanation is that the small-scale clinothems are fan-shaped in 3D, as is supported by obliquity variations, and that these clinothems are dip-parallel profiles located in lateral positions to fan apices.

Direct dip measurements and inference of lithologies and trajectories in this setting have limitations. During burial and compaction, differences in lithology within a sedimentary unit will cause differences in their appearance when resolved in seismic data. This process begins already at shallow burial, when successive clinothems cover their older equivalent during shelf platform progradation. The marked differences in dip-angles reported here suggest lithology contrasts that warrant differing decompaction coefficients for different clinothems. A clinothem-by-clinothem successive backstripping may improve restoration of thickness and dip, but is ultimately founded on seismic resolution and interpretations of rock volumes with poorly constrained lithologic composition. As an example, the vertical profile marked 1 in Figure 3a includes ~65% large-scale clinothem, and ~35% small-scale clinothem with high-angle foresets, without accounting for differences in velocity (Figure 3b). Their presumed differences in lithologic composition would return a reduced bulk net:gross value, a reduced thickness value after restoration, with correspondingly lower foreset angles.

As a whole, this alternating architecture of two nested clinof orm scales is indicative of how the overall progradation of intrashelf platforms sediments prograde; autocyclic compensational stacking occurs incrementally at different sediment delivery points along the platform margin, with slightly different directions. These recurring shifts in obliquity are evident in other intrashelf clinof orms also (Hodgson et al., 2018). The progradation rate was highest when the small-scale clinof orms developed, and the variation in clinof orm obliquity between sets reflects differences in local progradation direction and autocyclic compensation along the platform front. Alternating periods of lower sediment accumulation caused draping across the entire platform profile, and a presumed reduced intrashelf platform progradation rate, at least locally (Figure 3b). Where sediment delivery points overlap but differ in progradation direction, successive sets of different obliquity is discernible in seismic profiles. Jones et al. (2015) identified different platform-edge trajectories along contemporaneous, directly correlatable strata in the Karoo Basin, and warned against inferring basin development history from single 2D datasets. While beyond the scope of this study, an effort to laterally map related clinothem sets such as those outlined in Figure 1a may test this model further.

## 6 | CONCLUSIONS

- Intrashelf platform growth occurs in progradational pulses interrupted by draping of strata over its bathymetric profile, leading to nested clinof orm architecture.
- The platform-scale clinothems may develop during flooding periods, or when depositional focus is directed elsewhere along the intrashelf platform front.
- Subtle differences in obliquity between sets of small-scale clinof orms demonstrate that compensational stacking occurs along the platform front.
- Any inferences on lithology or comparisons to other studies need to consider maximum burial depth and lithologic composition prior to restoration.

## ACKNOWLEDGEMENTS

The authors thank TGS, WGPS, and VBPR for providing seismic data and allowing data use in this publication. We acknowledge support from the Research Centre for Arctic Petroleum Exploration (ARCEX), funded by the Research Council of Norway (grant number 228107) together with ten academic and nine industry partners, and the Centre for Earth Evolution and Dynamics (CEED) funded by the Research Council of Norway through their Centre of Excellence grant 223272. Henrik Stokke and Romain Corseri are acknowledged for their helpful provision of data. Comments from Miquel Poyatos-Moré and constructive reviews from M. Smelror, A. Ryseth and one anonymous reviewer has refined the manuscript. There are no conflicts of interest to report for this work.

## ORCID

Ivar Midtkandal  <https://orcid.org/0000-0002-4507-288X>

Jan Inge Faleide  <https://orcid.org/0000-0001-8032-2015>

Sverre Planke  <https://orcid.org/0000-0001-6128-2193>

## REFERENCES

- Allen, P. A., & Allen, J. R. (2013). *Basin analysis: Principles and application to petroleum play assessment* (3rd ed., p. 632). New York: Wiley-Blackwell.
- Anell, I., & Midtkandal, I. (2017). The quantifiable clinothem - types, shapes and geometric relationships in the Plio-Pleistocene Giant Foresets Formation, Taranaki Basin, New Zealand. *Basin Research*, 29, 277–297. <https://doi.org/10.1111/bre.12149>
- Baig, I., Faleide, J. I., Jahren, J., & Mondol, N. H. (2016). Cenozoic exhumation on the southwestern Barents Shelf: Estimates and uncertainties constrained from compaction and thermal maturity analyses. *Marine and Petroleum Geology*, 73, 105–130.
- Corseri, R., Faleide, T. S., Faleide, J. I., Midtkandal, I., Serck, C. S., Trulsvik, M., & Planke, S. (2018). A diverted submarine channel of

- Early Cretaceous age revealed by high-resolution seismic data, SW Barents Sea. *Marine and Petroleum Geology*, 98, 462–476.
- Døssing, A., Jackson, H. R., Matzka, J., Einarsson, I., Rasmussen, T. M., Olesen, A. V., & Brozena, J. M. (2013). On the origin of the Amerasia Basin and the High Arctic Large Igneous Province—Results of new aeromagnetic data. *Earth and Planetary Science Letters*, 363, 219–230.
- Grundvåg, S.-A., Marin, D., Kairanov, B., Śliwińska, K. K., Nøhr-Hansen, H., Jelby, M. E., ... Olaussen, S. (2017). The Lower Cretaceous succession of the northwestern Barents Shelf: Onshore and offshore correlations. *Marine and Petroleum Geology*, 86, 834–857.
- Helland-Hansen, W., & Hampson, G. J. (2009). Trajectory analysis: Concepts and applications. *Basin Research*, 21(5), 454–483.
- Henriksen, E., Bjornseth, H. M., Hals, T. K., Heide, T., Kiryukhina, T., Klovjan, O. S., ... Stoupakova, A. (2011). Uplift and erosion of the greater Barents Sea: impact on prospectivity and petroleum systems. In A. M. Spencer, A. F. Embry, D. L. Gautier, A. V. Stoupakova, & K. Sørensen (Eds.), *Arctic Petroleum Geology* (pp. 271–281). London, UK: Geological Society of London
- Hodgson, D. M., Browning, J. V., Miller, K. G., Hesselbo, S. P., Poyatos-Moré, M., Mountain, G. S., & Proust, J.-N. (2018). Sedimentology, stratigraphic context, and implications of Miocene intrashelf bottomset deposits, offshore New Jersey. *Geosphere*, 14, 95–114. <https://doi.org/10.1130/GES01530.1>
- Jones, G. E. D., Hodgson, D. M., & Flint, S. S. (2015). Lateral variability in clinoform trajectory, process regime, and sediment dispersal patterns beyond the shelf-edge rollover in exhumed basin margin-scale clinoforms. *Basin Research*, 27(6), 657–680. <https://doi.org/10.1111/bre.12092>
- Klausen, T. G., & Helland-Hansen, W. (2018). Methods for restoring and describing ancient clinoform surfaces. *Journal of Sedimentary Research*, 88(2), 241–259.
- Lebedeva-Ivanova, N., Polteau, S., Bellwald, B., Planke, S., Berndt, C., & Stokke, H. H. (2018). Toward one-meter resolution in 3D seismic. *The Leading Edge*, 37(11), 818–828.
- Marcussen, Ø., Faleide, J. I., Jahren, J., & Bjørlykke, K. (2010). Mudstone compaction curves in basin modelling: A study of Mesozoic and Cenozoic Sediments in the northern North Sea. *Basin Research*, 22(3), 324–340. <https://doi.org/10.1111/j.1365-2117.2009.00430.x>
- Midtkandal, I., Faleide, J. I., Faleide, T. S., Serck, C. S., Planke, S., Corseri, R., ... Nystuen, J. P. (in press). Lower Cretaceous Barents Sea strata: Epicontinental basin configuration, timing, correlation, and depositional dynamics. *Geological Magazine*.
- Midtkandal, I., & Nystuen, J. P. (2009). Depositional architecture of a low-gradient ramp shelf in an epicontinental sea: The lower Cretaceous of Svalbard. *Basin Research*, 21(5), 655–675. <https://doi.org/10.1111/j.1365-2117.2009.00399.x>
- Mountain, G., & Proust, J.-N. (2010, September 10). The New Jersey margin scientific drilling project (IODP Expedition 313): Untangling the record of global and local sea-level changes. *Scientific Drilling*, 10, 26–34. <https://doi.org/10.2204/iodp.sd.10.03.2010>
- Patruno, S., Hampson, G. J., & Jackson, C. A. L. (2015). Quantitative characterisation of deltaic and subaqueous clinoforms. *Earth-Science Reviews*, 142, 79–119.
- Patruno, S., & Helland-Hansen, W. (2018). Clinoforms and clinoform systems: Review and dynamic classification scheme for shorelines, subaqueous deltas, shelf edges and continental margins. *Earth-Science Reviews*, 185, 202–233. <https://doi.org/10.1016/j.earscirev.2018.05.016>
- Poyatos-Moré, M., Jones, G. E. D., Brunt, R. L., Hodgson, D. M., Wild, R. J., & Flint, S. S. (2016). Mud-dominated basin-margin progradation: Processes and implications. *Journal of Sedimentary Research*, 86(8), 863–878.
- Rüpke, L. H., Schmalholz, S. M., Schmid, D. W., & Podladchikov, Y. Y. (2008). Automated thermotectonostratigraphic basin reconstruction: Viking Graben case study. *AAPG Bulletin*, 92(3), 309–326.
- Sclater, J. G., & Christie, P. A. F. (1980). Continental stretching: An explanation of the Post-Mid-Cretaceous subsidence of the central North Sea Basin. *Journal of Geophysical Research: Solid Earth*, 85(B7), 3711–3739.
- Smelror, M., Larssen, G. B., Olaussen, S., Rømuld, A., & Williams, R. (2019). Late Triassic to Early Cretaceous palynostratigraphy of Kong Karls Land, Svalbard, Arctic Norway, with correlations to Franz Josef Land, Arctic Russia. *Norwegian Journal of Geology*, 98(4), 1–31.
- Smelror, M., Mørk, A., Monteil, E., Rutledge, D., & Leereveld, H. (1998). The Klippfisk formation—a new lithostratigraphic unit of Lower Cretaceous platform carbonates on the Western Barents Shelf. *Polar Research*, 17(2), 181–202.
- Worsley, D., Johansen, R., & Kristensen, S. E. (1988). The mesozoic and cenozoic succession of Tromsøflaket. *Norwegian Petroleum Directorate Bulletin*, 4(4), 42–65.

**How to cite this article:** Midtkandal I, Faleide TS, Faleide JI, Planke S, Anell I, Nystuen JP. Nested intrashelf platform clinoforms—Evidence of shelf platform growth exemplified by Lower Cretaceous strata in the Barents Sea. *Basin Res.* 2019;00:1–8. <https://doi.org/10.1111/bre.12377>